Nucleic Acids Research, 1999, Vol. 27, No. 2 517–525

Increased nuclear factor 1 binding to its nucleosomal site mediated by sequence-dependent DNA structure

Patrik Blomquist+, Sergey Belikov[1] and Örjan Wrange*

Laboratory of Molecular Genetics, Department of Cell and Molecular Biology, Medical Nobel Institute, Karolinska Institute, S-171 77 Stockholm, Sweden and [1]W. A. Engelhardt Institute of Molecular Biology, Russian Academy of Sciences, Moscow 117984, Russia

Received September 28, 1998; Revised and Accepted November 10, 1998

ABSTRACT

The organization of DNA into chromatin is important in the regulation of transcription, by influencing the access of transcription factors to their DNA binding sites. Nuclear factor 1 (NF-1) is a transcription factor which binds to DNA constitutively and which interacts with its cognate DNA site with high affinity. However, this affinity is drastically reduced, ~100- to 300-fold, when the binding site is organized into a nucleosome. Here we demonstrate that the introduction of stretches of adenines of length 5 nt (A-tracts) on both sides of the NF-1 binding site has a distinct effect on NF-1 binding to a nucleosomal, but not to a free, NF-1 binding site. The position of the A-tracts, relative to the rotational phase of a synthetic DNA bending sequence, the TG-motif, decides whether the NF-1 affinity increases or decreases. The NF-1 binding affinity is seven times stronger when the flanking A-tracts are positioned out-of-phase with the TG-motif than it is when the A-tracts are positioned in-phase with the TG-motif. We demonstrate that this effect correlates with differences in DNA curvature and apparent histone octamer affinity. We conclude that DNA curvature influences the local histone–DNA contacts and hence the accessibility of the NF-1 site in a nucleosome context.

INTRODUCTION

Recognition of specific binding sites in DNA by transcription factors is the initial step in the induction of gene expression. In the living cell, the DNA is organized as chromatin whose basic structural unit is the nucleosome (1). Current belief is that the packaging of DNA into chromatin represses gene expression by limiting the access of transcription factors to their specific DNA sites (2). *In vitro* studies have examined how the organization of DNA within a nucleosome affects the access of transcription factors. Some factors interact with nucleosomal DNA with affinities that are only slightly lower than their affinities for free DNA. Examples of this are the glucocorticoid receptor (GR) (3–5), the progesterone receptor (6), the thyroid hormone receptor (7) and Fos/Jun (8). Other factors such as Gal4, c-Myc, heat shock factor, SP1 and TFIIIA bind nucleosomal DNA with an affinity at least one order of magnitude lower than their affinity for free DNA (9–11). Another class of factors has an even lower affinity for nucleosomal DNA, by at least two orders of magnitude. Nuclear factor 1 (NF-1) (4,12–14) and TBP (15,16) belong to this category.

The NF-1 family of transcription factors participates in transcriptional regulation of a great number of genes in many different cell types (17). The family is encoded by four different genes (18) and further diversity is created by differential splicing (18,19). All NF-1 proteins bind as homodimers to DNA in the major groove and recognize a partially palindromic consensus DNA sequence TGGA/C(N)$_5$GCCAA (20). The N-terminal domain of NF-1 is the domain which binds to DNA. It is highly conserved and shows no homology to any of the other known classes of DNA binding motifs (21,22).

In several promoters, the NF-1 binding site is close to the binding site(s) of other transcription factors (17,23,24). One example of this is the mouse mammary tumor virus (MMTV) promoter, where the NF-1 binding site is next to several binding sites for the GR (17). In the living cell this NF-1 site is only occupied after glucocorticoid hormone stimulation (25,26). It has been suggested that the chromatin organization of the DNA prevents NF-1 from binding to the uninduced MMTV promoter, i.e. in the absence of bound GR (25). This hypothesis is supported by *in vitro* studies demonstrating that the affinity of NF-1 for the MMTV promoter is drastically decreased when the DNA segment which contains the NF-1 binding site is reconstituted into nucleosomes (4,12,14,27). The NF-1 binding site in the MMTV promoter is rotationally positioned so that its major grooves face the histone octamer. This has been shown both *in vitro* (4) and *in vivo* (26). However, *in vitro* studies have demonstrated that the low affinity of NF-1 for its nucleosomal binding site does not depend on the translational or rotational positioning of the NF-1 site, but is an inherent property of the NF-1 protein (13,14,27). In the former study we vaired the rotational positioning of the nucleosomal NF-1 site by placing it into two different rotational frames relative to a synthetic DNA bending sequence, the TG-motif (28). The TG-motif was used to direct the rotational setting of the nucleosomal DNA.

The nucleotide sequence affects nucleosome stability through its effect on the curvature and bendability of DNA (29). We wondered to what extent the flanking DNA sequence context of an NF-1 binding site influences its affinity for NF-1. A-tracts are straight and rigid and thus they affect DNA curvature and influence histone–DNA contacts in nucleosomes (30). We

*To whom correspondence should be addressed. Tel: +46 8 728 7373; Fax: +46 8 31 3529; Email: orjan.wrange@cmb.ki.se

+Present address: Department of Molecular Biology and Genomics, Pharmacia and Upjohn, S-112 87 Stockholm, Sweden

decided to try to destabilize histone–DNA contacts around the nucleosomal NF-1 site by positioning of A-tracts next to the NF-1 binding site and to evaluate the effect on NF-1 binding.

Here we show that A-tracts of length 5 bp placed on both sides of an NF-1 binding site may either increase or decrease its affinity for NF-1. The NF-1 binding affinity increased when the A-tracts were positioned out-of-phase relative to the A/T triplets of the surrounding DNA-bending sequence, i.e. the TG-motif. Conversely, NF-1 binding decreased when the A-tracts were positioned in rotational phase with the TG-motif. These effects on NF-1 binding affinity correlated with the effect of DNA sequence on both DNA curvature and histone octamer affinity. We conclude that nucleosomal DNA accessibility can be drastically modulated by flanking DNA sequences. This may have been exploited in the evolution of different promoter strengths, for example, and in this way it may moderate gene expression.

MATERIALS AND METHODS

Plasmid constructions

We have previously described the construction of plasmids which contain a single transcription factor binding site in the synthetic DNA-bending sequence referred to as the TG-motif (5). Plasmids No4 and Ni4 have been described elsewhere (13). All DNA segments which were used for construction were obtained from synthetic oligonucleotides. ANoA3.5 was constructed by cloning a 40 bp DNA segment containing a TG-motif and an NF-1 binding site flanked by -TTTTT- upstream and -AAAAA- downstream (ANoA, the sequence of the top strand is shown in Fig. 1A). The NF-1 site was derived from the MMTV promoter (13). The DNA segments were cloned into the asymmetric *Ava*I site of plasmid pGemQ2 (5). The 40 bp of ANoA was followed by three 20 bp DNA segments of the synthetic DNA-bending sequence referred to as the TG-motif (28) (TG) and a 10 bp DNA segment of DNA-bending sequence, half a TG-motif (hTG). Hence a total number of 3.5 TG repeats were inserted after the ANoA segment. ANiA3.5 differed from ANoA3.5 only in that the NF-1 binding sequence with the flanking A-tracts was moved 5 bp upstream relative to the DNA-bending sequence (the sequence of the top strand is shown in Fig. 1A) which caused rotation by 180° of the NF-1 site relative to the TG-motif. These DNA constructs were cut out from their parental plasmids as 161 bp long *Eco*RI–*Hin*dIII DNA fragments which were used for nucleosome reconstitution. To be precise, these inserts contained 157 bp of double-stranded DNA and 4 nt of 5′-protruding DNA at each end. The first nucleotide in the top strand, the *Eco*RI site, was given number 1.

Nucleosome reconstitution

DNA end-labeling with [γ-^{32}P]ATP and fragment isolation have been described previously (3,5). Nucleosome reconstitution and purification of *in vitro* reconstituted mononucleosomes by glycerol gradient centrifugation were performed as described previously (3) but with two modifications, a 7–30% glycerol gradient was used instead of a 5–30% gradient and the glycerol gradients contained 10 µg/ml purified bovine serum albumin instead of insulin.

NF-1 binding and mapping of nucleosomal positioning

Exonuclease III digestion, DNase I footprinting and DMS methylation protection were performed as previously described (13). Quantification of NF-1 binding was done with a PhosphorImager™ and ImageQuant™ software (Molecular Dynamics). Reference bands were used to compensate for variations in sample loading and DNase I digestion or DMS methylation.

Preparation of NF-1

Recombinant NF-1 was prepared from HeLa cells infected with vaccinia virus that contained a full-length clone for NF-1 with six histidine residues fused to the N-terminus (31). The NF-1 was purified using Ni^{2+}–NTA–agarose, as described previously (13).

Analysis of nucleosomes by electrophoretic mobility shift assay

The amount of free DNA in the nucleosomes was analyzed by electrophoretic mobility shift assay. 5000 c.p.m. of probe, either free or nucleosomal, was diluted to 20 µl with GR binding buffer (20 mM Tris–HCl, pH 7.6, 1 mM Na_2EDTA, 10% v/v glycerol, 50 mM NaCl, 5 mM DTT, 0.1 mg/ml bovine serum albumin) containing bromophenol blue to a final concentration of 0.0125% and analyzed on 4% non-denaturing acrylamide gels (5). The amount of free DNA was quantified by the use of a PhosphorImager™ and ImageQuant™ software (Molecular Dynamics).

DNA curvature

The program BEND was used to calculate sequence-dependent curvature (32). In this program, the specific curvature at base pair N is defined as the angle between normal vectors at base pairs N–15 and N+15.

Relative histone octamer affinity assay

Aliquots of 0.5 pmol of each of the 161 bp *Eco*RI–*Hin*dIII fragments from No4, ANoA3.5 and ANiA3.5, each one 5′-end-labeled with T4 polynucleotide kinase at the *Hin*dIII site, were mixed. These were used in each of three parallel *in vitro* nucleosome reconstitutions (above) but with the indicated amounts of long chromatin in the reconstitution mix. Chromatin was quantified at 260 nm where 1 OD unit equals 50 µg of chromatin. We used less long chromatin than is normally used for *in vitro* nucleosome reconstitution; 0.5, 0.17 and 0.06 times. The mononucleosomal DNA was recovered by extraction with phenol/chloroform (2:1) and precipitation by ethanol in the presence of 5 µg *Escherichia coli* tRNA as carrier. The recovered DNA was cleaved with *Hin*fI and then re-extracted with phenol/chloroform 2:1 and ethanol precipitated. Pellets were dried and dissolved in loading buffer, separated on a denaturing polyacrylamide gel and the relative amount of each DNA fragment in the mononucleosomal fraction was quantified by PhosphorImager analysis. This was then compared with the relative amounts in the original DNA mix which had been used for nucleosome reconstitution.

RESULTS

Effects of A-tracts on nucleosomal position

We have shown previously that the transcription factor NF-1 binds to a nucleosomal DNA binding site with 100–300 times lower affinity than it binds to free DNA. This strong decrease in NF-1 affinity does not depend on the translational or the rotational position of the NF-1 binding site relative to the histone octamer

surface (13). In these experiments we used fragments of DNA which were 161 bp long and which harbored a 95 bp DNA segment based on the 20 bp repetitive synthetic DNA-bending sequence, the TG-motif. This arrangement directed the positioning of the NF-1 binding site in the nucleosome (28). The TG-motif consists of triplets of G/C and A/T which are placed 5 bp apart with a 10 bp periodicity (Fig. 1A). When the TG-motif is reconstituted into a nucleosome *in vitro*, it will preferentially bend in one direction such that the G/C triplets are located where minor grooves face the periphery and the A/T triplets face the histone octamer (28).

We wondered to what extent the nucleosomal inhibition of NF-1 binding could be counteracted by a change of the local sequence context around the NF-1 site. Our first attempt to address this was to replace an AGCCT segment with a TAAAA segment immediately downstream of the NF-1 binding site in the construct No4 (No4 is shown in Fig. 1B). This resulted in deletion of one GCC triplet in the TG-motif of No4 and the introduction of an A/T-rich segment which interrupted the periodicity of the TG-motif. The same approach has been shown previously to disturb histone–DNA contacts and to improve the accessibility of a nucleosomal glucocorticoid receptor binding site (5). However, the constructs we obtained in this way did not have any detectable effect on NF-1 binding as monitored by DNase I footprinting and by DMS methylation protection analysis (data not shown).

This prompted us to introduce 5 bp of homopolymeric A-tracts both upstream and downstream of the NF-1 binding site to produce an NF-1 binding segment that we called ANoA or ANiA (Fig. 1A). The NF-1 binding site was positioned in two opposite rotational frames with respect to the preferred rotational positioning of the TG-motif (Fig. 1A), 'No' for facing out and 'Ni' for facing in. The two constructs ANoA3.5 and ANiA3.5 (Fig. 1B) should therefore have the two consecutive major grooves of the NF-1 binding site facing outwards or inwards, respectively, relative to the histone octamer surface. This would only be true if the rotational position of the nucleosome was dictated by the TG-motif. The design of the constructs resulted in two 7 bp A-tracts in ANoA3.5 and two 8 bp A-tracts in ANiA3.5 (Fig. 1A). Nucleosomes were reconstituted *in vitro* by salt dilution (3) and the mononucleosomes were purified by glycerol gradient centrifugation. This routinely gave nucleosome preparations in which >95% of the DNA was organized in nucleosomes according to analysis by electrophoretic mobility shift assay (Fig. 1C). In these analyses we noted that the relative amount of free DNA was lower in the ANiA3.5 mononucleosome preparations than in the other two nucleosomal constructs (Fig. 1C).

The rotational position of the DNA in the different nucleosomes was evaluated by comparing the DNase I footprinting patterns (Fig. 2). Both nucleosomal No4 and ANiA3.5 showed a characteristic 10 bp repeated DNase I pattern (Fig. 2A and B shows top strand and bottom strand, respectively) which is typical of DNA rotationally positioned on a histone octamer surface (33). The DNase I pattern of nucleosomal ANoA3.5, however, was more complex. It showed several nucleosome-dependent alterations in the DNase I cutting pattern, including cut sites which were more frequent than the 10 bp ladder seen in the other two constructs. We interpret the ANoA3.5 pattern as arising from several superimposed nucleosome patterns caused by several different rotational positions of ANoA3.5. This interpretation was confirmed by aligning the results of the DNase I footprinting in a sequence diagram (Fig. 2C). No4 and ANiA3.5 clearly had

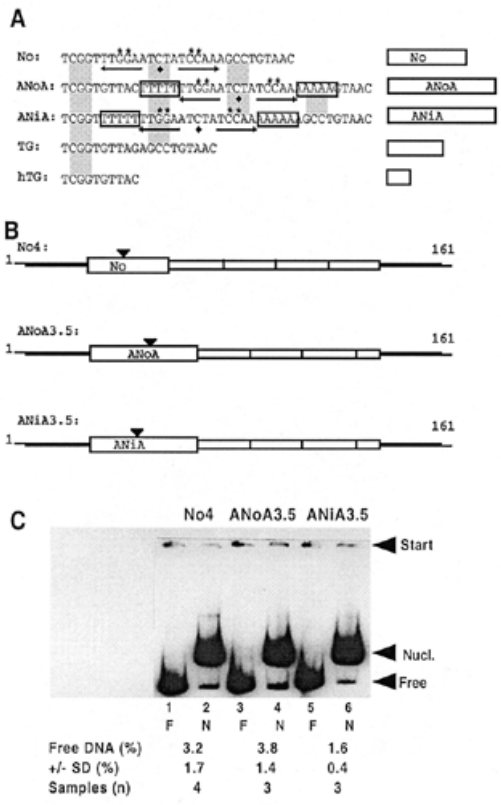

Figure 1. DNA sequences, DNA segments and reconstituted nucleosomes. (**A**) The top strand is shown for the annealed double-stranded oligonucleotides used in the construction of the DNA segments. NF-1 half-sites are indicated by arrows and the dyad of the NF-1 site is represented by a diamond below the sequence. Stars indicate G-C bp in which the G residue is protected from dimethyl sulfate (DMS) methylation upon NF-1 binding. A(T)-tracts flanking the NF-1 site in ANoA3.5 and ANiA3.5 are indicated by boxes. Gray areas indicate the positions of G/C triplets in the TG-motif. If the TG-motif directs the rotational position in the nucleosome, this would correspond to positions of the minor grooves facing out. Note the position of the A-tracts in ANoA3.5 and ANiA3.5 compared with these gray areas. Symbols for the different DNA segments in (B) are shown to the right. (**B**) 161 bp *Eco*RI–*Hin*dIII DNA fragments No4, ANoA3.5 and ANiA3.5 used for *in vitro* reconstitution of nucleosomes are shown. Symbols are as in (A). Thin lines indicate vector sequences and black triangles indicate positions of the *Hin*fI site in each construct. Positions 1 and 161 are indicated. (**C**) Free (F) or nucleosomal (N) DNA analyzed by electrophoretic mobility shift assay. The average amounts of free DNA in the nucleosomal fractions are shown as a percentage with standard deviation (± SD). *n* indicates the number of experiments. Start indicates the start of electrophoresis.

the expected rotational positioning with the G/C triplets of the TG-motif positioned where the minor grooves are facing outwards (gray areas in Fig. 2C are flanked by DNase I cuts). This was also true for one population of DNase I cut sites in ANoA3.5 and, in addition, there were other nucleosomally induced cut sites in this construct that showed a different distribution (open arrowheads in Fig. 2C).

The translational position of DNA in the different nucleosomes was evaluated by exonuclease III protection analysis (5). In a uniquely positioned nucleosome the location of the first histone-induced exonuclease III stop on either DNA strand defines the nucleosomal borders; a nucleosome is known to cover 144–146 bp. Exonuclease III digestion also gives rise to internal nucleosome-dependent stops spaced by 10 bp due to the histone–DNA contacts formed once per helical turn of DNA (34). Each strand

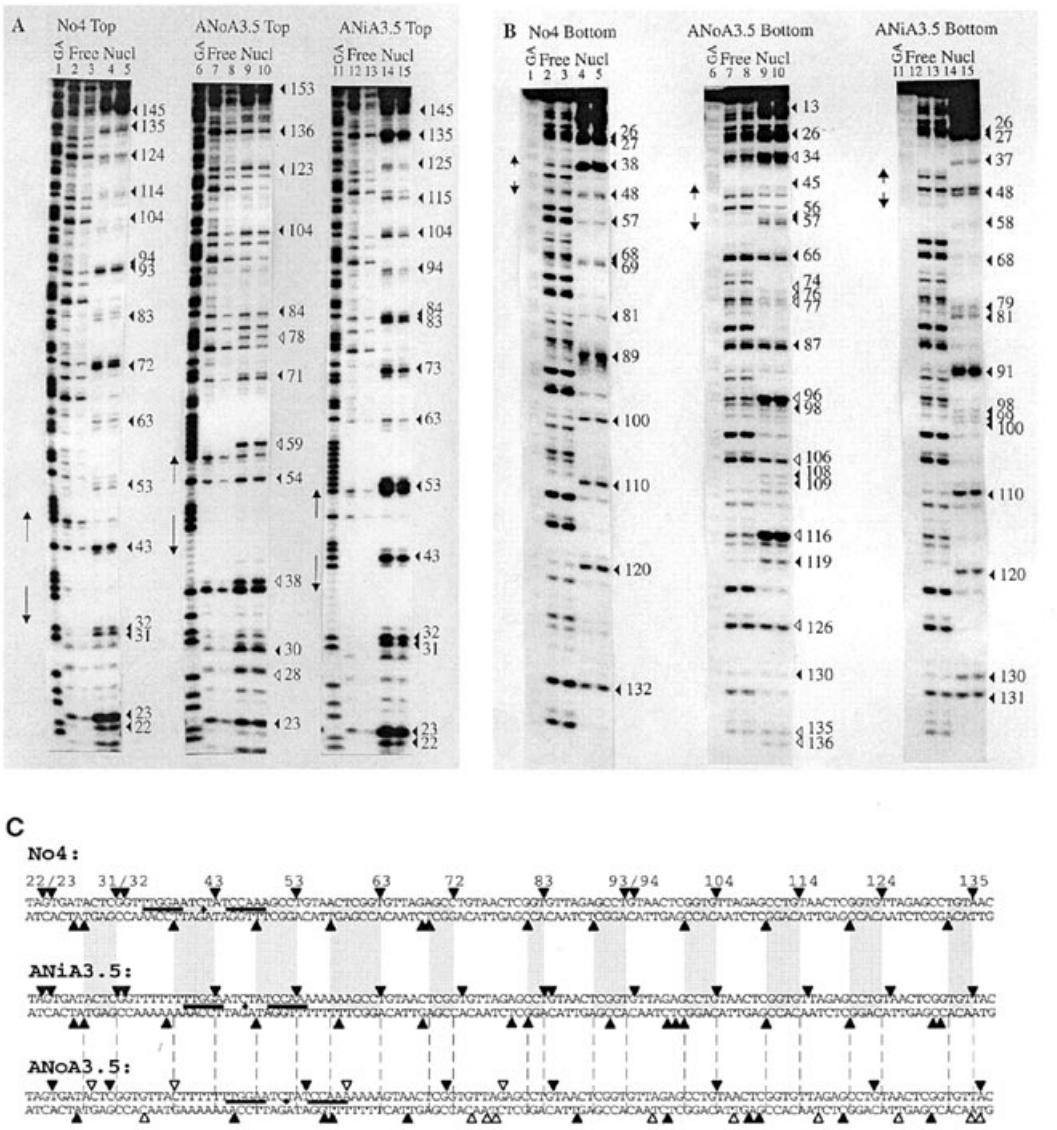

Figure 2. Rotational position of nucleosomal DNA analyzed by DNase I footprinting. (**A**) Free (Free) and nucleosomal (Nucl) DNA with the top strand 5′-end-labeled was digested with DNase I. GA indicates the G+A sequence lane. Vertical arrows indicate NF-1 half-sites. Black arrowheads indicate nucleosomally induced DNase I cuts. Open arrowheads in ANoA3.5 indicate nucleosomally induced DNase I cuts that differ significantly from No4 and ANiA3.5. Numbers indicate the position downstream of the DNase I cuts. (**B**) DNase I digestion of free and nucleosomal DNA with the bottom strand 5′-end-labeled. Symbols are as in (A). (**C**) Graphic representation of the DNase I cuts in nucleosomal DNA, a summary from several experiments similar to the ones shown in (A) and (B). The sequences are shown from position 20 to 139. Arrowheads, filled and open, indicate DNase I cuts as in (A) and (B). The numbers refer to cut sites in the top strand of No4. Gray areas indicate minor grooves facing out in No4 and ANiA3.5 as determined by DNase I digestion. Dotted lines indicate minor grooves facing out in ANoA3.5, if positioned rotationally as No4 and ANiA3.5. NF-1 half-sites are indicated by horizontal lines and dyads of NF-1 sites are indicated by diamonds.

of No4 and ANiA3.5 gave rise to several nucleosomally induced exonuclease III stops spaced by 10 bp (Fig. 3A and B). As we had earlier found (13), No4 adopted one translational position, with the dyad of the NF-1 binding site positioned 50 bp from the nucleosome pseudo-dyad (Fig. 3C). ANiA3.5 adopted two different translational positions, but with the same rotational position and with a distance of 45 or 35 bp between the dyad of the NF-1 binding site and the nucleosomal pseudo-dyad. ANoA3.5, on the other hand, again showed a more complex pattern of nucleosomally induced exonuclease III cut sites, which suggests the existence of several different rotational and translational positions (Fig. 3C summarizes our interpretation of the exonuclease III analysis).

From the exonuclease III protection and DNase I footprinting analyses we conclude that ANoA3.5 adopts several translational and rotational positions, while No4 and ANiA3.5 have unique rotational positions, although the latter adopts two translational positions separated by 10 bp. A probable reason for the occurrence of several rotational positions of the ANoA3.5 nucleosome is that the two A-tracts in ANoA3.5 oppose and to some extent override the capacity of the TG-motif to determine the rotational position of the nucleosomal DNA.

A-tracts modulate the binding affinity of NF-1 to nucleosomal DNA

NF-1 binding to the different DNA constructs, both free and nucleosomal, was analyzed by DMS methylation protection (Fig. 4) and by DNase I footprinting (Fig. 5). We have shown previously that nucleosomal NF-1 binding can be monitored by DMS methylation protection with high specificity (13). No DMS methylation protection which depended on NF-1 was seen outside the NF-1 binding site, even with a large excess of NF-1 (Fig. 4 and data not shown). This is in contrast to DNase I footprinting where non-specific interaction outside the NF-1 binding site often influences the footprinting pattern. However, one advantage with DNase I footprinting is that it allows concomitant monitoring of the histone–DNA interactions in the nucleosome during the binding reaction (Fig. 5). Histone–DNA contacts do not show any protection from DMS methylation (13,35).

Table 1. Relative NF-1 binding affinity to nucleosomal DNA constructs, calculated as the concentration of NF-1 protein needed to saturate the different nucleosomal constructs to 50% divided by the concentration of NF-1 protein needed to give 50% protection in corresponding free DNA constructs

DNA construct	Relative NF-1 binding affinity[a] (nucleosomal/free DNA)
ANoA3.5	42-fold
No4	71-fold
ANiA3.5	280-fold

[a]Expressed as the fold increase in concentration of NF-1 for binding to nucleosomal DNA as compared with free DNA.

Experiments in which increasing amounts of NF-1 protein were incubated with a constant amount of free or nucleosomal DNA showed that all DNA constructs when present in free DNA bound NF-1 with similar affinities (Fig. 6, filled symbols). The small differences in NF-1 binding affinity seen for the free DNA are not significant, as indicated by the overlapping error bars representing the standard deviations of the analysis. When the three DNA constructs were organized into nucleosomes, their binding affinities for NF-1 were different (Fig. 6, empty symbols). In this case NF-1 bound to nucleosomal ANoA3.5 with significantly higher affinity than to nucleosomal No4. This was clearly seen by DMS methylation protection (Fig. 6). There was a tendency for the same difference in affinity also when analyzed by DNase I footprinting (data not shown), but the difference was not statistically significant. Nucleosomal ANiA3.5 showed a significantly lower affinity for NF-1 than nucleosomal No4 (indicated by stars in Fig. 6) and ANoA3.5. This difference was again only detectable by DMS methylation protection and was not seen with DNase I footprinting (data not shown). We estimated the relative affinity of NF-1 for the different nucleosomal DNA constructs from Figure 6. The amount of NF-1 protein needed to saturate the different nucleosomal constructs to 50% was calculated, relative to the amount needed to give 50% protection in free DNA. The results are presented in Table 1 and show that ANoA3.5 has a 7-fold higher affinity for NF-1 than ANiA3.5. We conclude that different nucleosomal sequence contexts have significant effects on NF-1 binding affinity. The reason for this is discussed below.

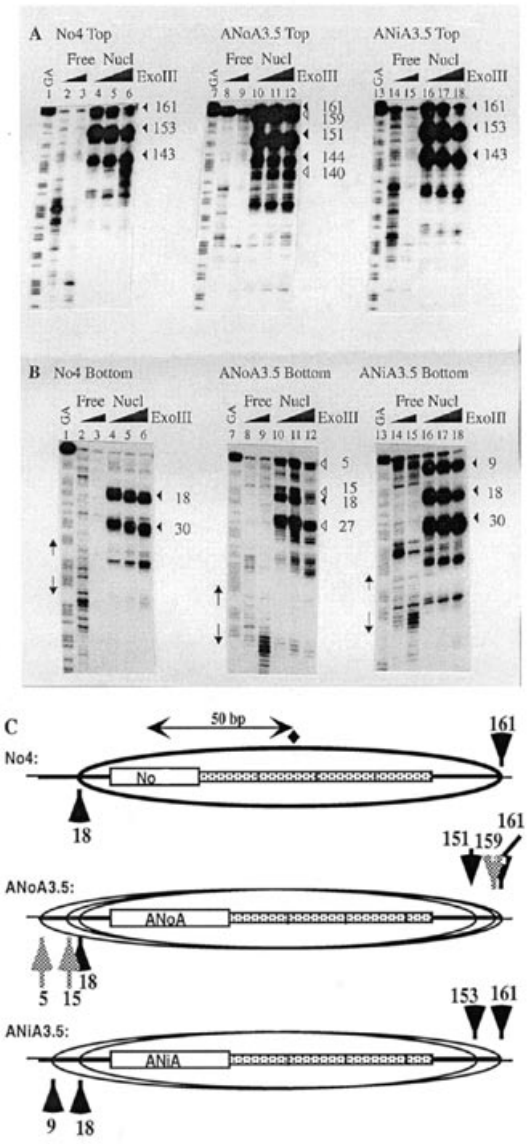

Figure 3. Translational position of nucleosomal DNA. (**A**) Exonuclease III digestion of free (Free) and nucleosomal (Nucl) 5′-end-labeled DNA (top strand). GA indicates the G+A sequence lane and black wedges above the lanes indicate increasing time of exonuclease III digestion. Triangles indicate nucleosome-induced exonuclease III stops and numbers indicate their positions. Open triangles indicate nucleosome-induced stops in ANoA3.5 that differ from No4 and ANiA3.5. (**B**) Exonuclease III digestion of free and nucleosomal 5′-end-labeled DNA (bottom strand). Vertical arrows indicate NF-1 half-sites. Other symbols are as in (A). (**C**) Graphic representation of the different populations of translationally positioned nucleosomes indicated by ellipsoids. Borders of the nucleosomal positions are shown as black arrows; gray arrows indicate positions in ANoA3.5 that differ from No4 and ANiA3.5. The diamond indicates the nucleosomal pseudo-dyad in No4. The distance to the dyad of the NF-1 site in No4 is given in bp and indicated by an arrow. The symbols for the different DNA constructs are as in Figure 1.

The difference in NF-1 affinity when comparing free and nucleosomal No4 agrees well with our previous results for this construct (13).

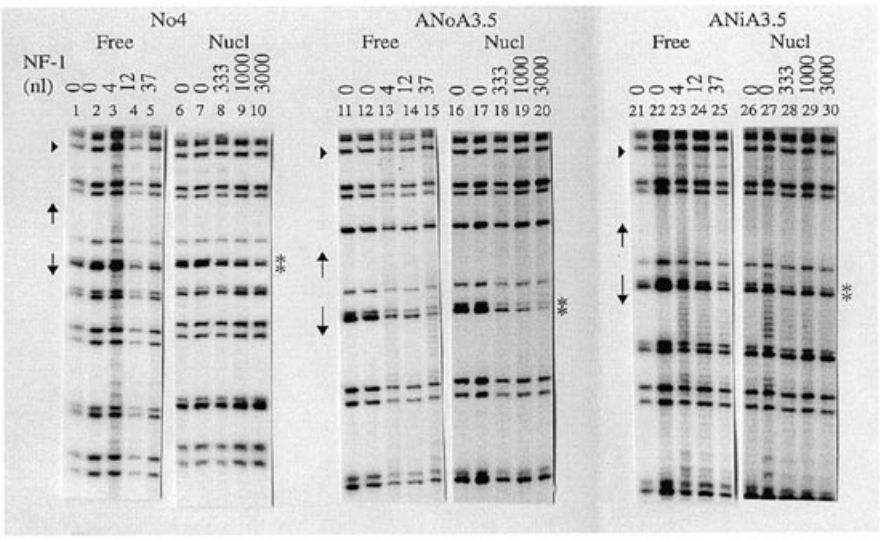

Figure 4. NF-1 binding monitored by DMS methylation protection analysis. Free (Free) and nucleosomal (Nucl) DNA fragments labeled in the bottom strand were incubated in the presence or absence of NF-1 and then subjected to DMS methylation. Lanes 1–10, No4; lanes 11–20, ANoA3.5; lanes 21–30, ANiA3.5. The amount in nl of NF-1 preparation added is indicated above each lane. The NF-1 binding sequence is indicated by vertical arrows and the two G residues that are protected from methylation by NF-1 are indicated by stars. The triangles indicate the reference bands used to compensate for variations in sample loading and DMS methylation.

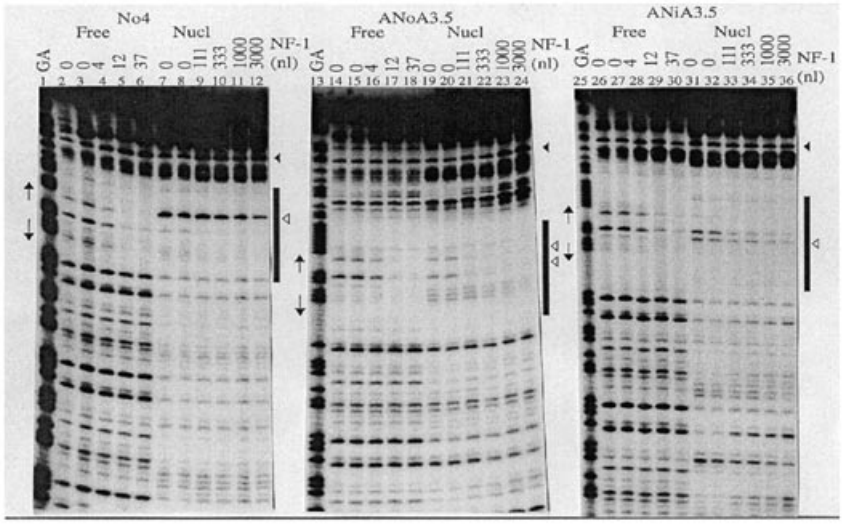

Figure 5. NF-1 binding monitored by DNase I footprinting analysis. Free (Free) and nucleosomal (Nucl) DNA fragments labeled on the bottom strand were incubated in the absence or presence of NF-1. The amounts of NF-1 are indicated as in Figure 4. GA indicates the G+A sequence lane and black triangles indicate reference bands used to compensate for variations in DNase I digestion and sample loading. Vertical arrows indicate the NF-1 binding site and the vertical black boxes indicate the NF-1-induced footprint. Lanes 1–12, No4; lanes 13–24, ANoA3.5; lanes 25–36, ANiA3.5. Open triangles indicate bands used for quantitation of NF-1 binding by PhosphorImager.

A-tracts positioned out-of-phase in a DNA-bending sequence interrupt DNA curvature and reduce histone octamer affinity

To evaluate the sequence-dependent curvature of the three NF-1 constructs we used a program BEND that calculates macroscopic curvature along a DNA sequence (32) using a bending model based on nucleosome positioning data (36). The program predicts significant curvature for No4 and ANiA3.5 constructs along the DNA fragment (Fig. 7). For ANoA3.5, it predicts a similar high level of DNA curvature for the 3′-part of the construct but a drastically reduced curvature is predicted for the 5′-region. Note that the curvature is reduced in two segments corresponding to the two flanking A-tracts of ANoA3.5 (the positions of the A-tracts are indicated by thick lines above the diagram in Fig. 7). In contrast, the curvatures of the A-tracts are higher in ANiA3.5 than the corresponding DNA segment in No4. In ANiA3.5 the A-tracts are moved 5 bp relative to the TG-motif and are thus in-phase with the A/T triplets of the TG-motif (Fig. 7).

We wondered whether the difference in DNA curvature has any effect on histone octamer–DNA affinity. This was addressed by

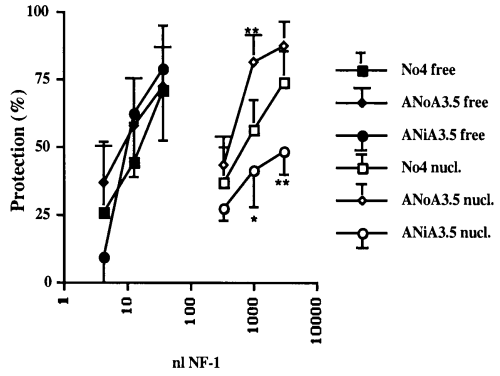

Figure 6. Graph showing quantification of binding of NF-1 analyzed by DMS methylation protection. Binding of NF-1 and standard deviations (error bars) are given in percent, where 100% means complete protection from DMS methylation. The curves for free (filled symbols) and nucleosomal DNA (open symbols) are indicated for each of the three constructs. * indicates a level of significance (P) < 0.05; **P < 0.01 (Student's t-test) for differences compared with No4.

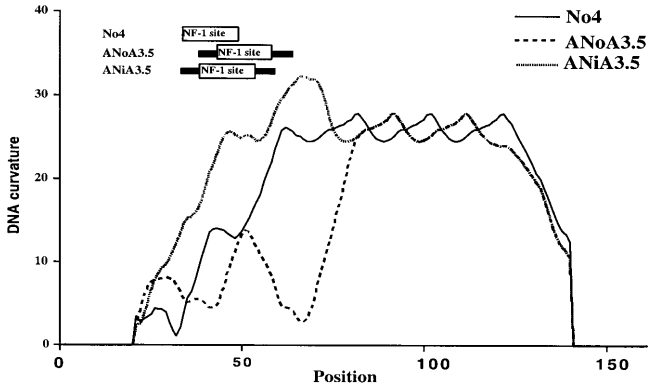

Figure 7. Analyses of the DNA curvature for the different constructs. The DNA curvature of the three constructs in angular degrees is plotted against the position (as defined in Fig. 1). Position of the NF-1 site (boxed) and the A-tracts (black bars) are indicated above the curves. The lines used for the different constructs are shown on the upper right. Note that the DNA curvature cannot be estimated for the 20 bp closest to the ends of the DNA due to program restrictions.

comparing the relative efficiencies of the constructs in binding to a histone octamer in a nucleosome reconstitution assay. In this assay equal amounts of the 161 bp *Eco*RI–*Hin*dIII fragments of the three DNA constructs were mixed and allowed to compete during *in vitro* nucleosome reconstitution. The amount of long chromatin, which we used as donor of histone octamers in the nucleosome reconstitution reaction, was titrated until it became limiting. Using this strategy the different amounts of each DNA fragment in the purified mononucleosome fraction would reflect their apparent relative affinity for histone octamer. The reconstituted mononucleosome fraction was recovered by glycerol gradient centrifugation (Fig. 8A). The DNA was extracted from the pooled mononucleosome fractions and cleaved with *Hin*fI (which cuts within the NF-1 binding site and generates a different fragment length for each construct; Fig. 1B). The DNA was then separated on a denaturing polyacrylamide gel and quantified by PhosphorImager analysis. As shown in Figure 8B, there was a reduction in the relative amount of the ANoA3.5 fragment as the histone octamer concentration was reduced in the nucleosome reconstitution mixture and a corresponding increase in the No4 DNA fragment. This shows that the apparent histone octamer–DNA affinity is reduced for the ANoA3.5 construct. This agrees with the DNA curvature analysis which showed that ANoA3.5 had a lower DNA curvature than the other constructs.

DISCUSSION

We have shown that A-tracts of 5 bp length flanking the NF-1 binding site can influence the binding of NF-1 to nucleosomal DNA. This effect was only seen in DNA organized into nucleosomes and depended strongly on the position of the A-tracts relative to the rotational phase of the surrounding DNA-bending sequence, the TG-motif. A-tracts are straight and rigid (32) and cause bending in the junctions between the A-tract and adjacent DNA (37) and hence here reported results are most likely caused by effects on histone–DNA interactions dictated by DNA structure.

Why does ANoA3.5 take up several rotational positionings? We favor the following explanation. The A-tracts in ANoA3.5 are out-of-phase with the A/T triplets of the TG-motif (Fig. 1A). Hence the two A-tracts in ANoA3.5 replace two triplets which in ANiA3.5 are a G/C triplet of the TG-motif and a TGG triplet in the NF-1 site (Fig. 1A, shadowed areas mark peripherally oriented minor grooves when directed by the TG-motif). In ANiA3.5, the two A-tracts are placed in the minor grooves which are oriented towards the octamer in the rotational position which is directed by the TG-motif. They are thus in perfect phase with the A/T triplets of the TG-motif (Fig. 1A). Shrader and Crothers have shown that replacing the G/C triplet of the TG-motif with a 5 bp A-tract results in strong reduction of nucleosome stability, while replacing the A/T triplet with a 5 bp A-tract, which then lies between the G/C triplets as in our construct ANiA3.5, has a less detrimental effect on nucleosome formation (38). Short A/T segments within nucleosomes are preferentially positioned in the minor grooves which face the histone octamer both *in vitro* (28) and *in vivo* (36). Our finding that ANoA3.5 is less stably organized in a nucleosome than ANiA3.5 agrees with previous results on the preferential rotational positioning of A/T segments in nucleosomes. Or, to rephrase it, the A-tracts which flank the NF-1 site in ANiA3.5 act in harmony with the direction of bending of the TG-motif, while the A-tracts of ANoA3.5 bend the DNA in the opposite direction to the TG-motif.

The higher affinity of NF-1 for its cognate binding site on the ANoA3.5 nucleosome cannot be explained solely by an opposite rotational DNA positioning of the NF-1 site relative to the ANiA3.5. We can make this conclusion since the control nucleosome No4 has a single rotational positioning with the major grooves of the NF-1 recognition sequence facing out, but still has a significantly lower NF-1 binding affinity than ANoA3.5. Our results suggest that the improved affinity of ANoA3.5 for NF-1 is caused by local destabilization of histone–DNA contacts around the NF-1 site. This destabilization is due to the out-of-phase position of the A-tracts relative to the TG-motif. This means that DNA cannot wrap so smoothly around the histone octamer (32). Furthermore, since bending occurs at the junction of an A-tract and adjacent B-DNA (37), we propose that the lower DNA curvature in ANoA3.5 compared with ANiA3.5 is due to an antagonistic DNA bending direction in the

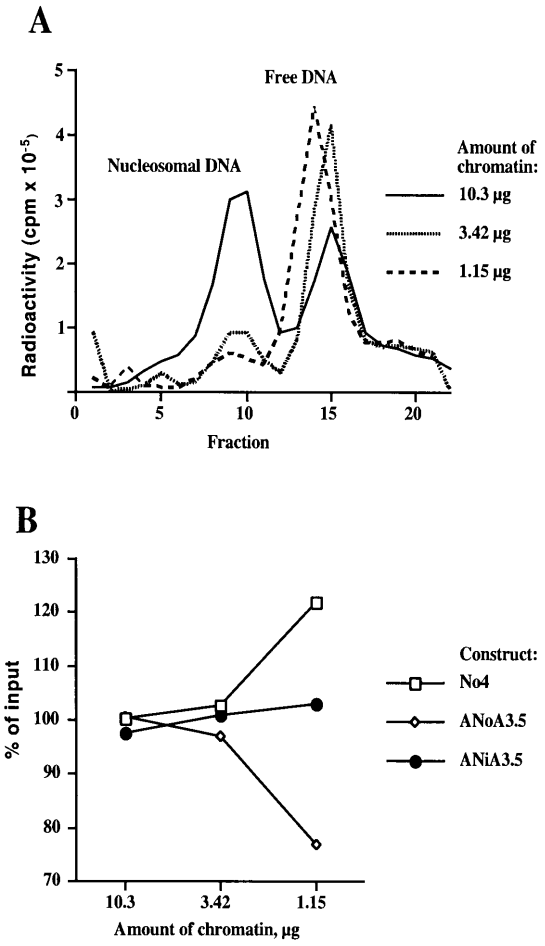

Figure 8. Relative histone octamer binding during nucleosome reconstitution. (**A**) Glycerol gradient profiles of simultaneous reconstitution of the three constructs using limiting amounts of long chromatin. The total amounts of chromatin used in the different nucleosome reconstitutions are indicated to the right side of the curves. (**B**) The amounts of nucleosomal DNA for the different constructs relative to the input DNA were plotted against the amount of chromatin used in the reconstitution; data points represent the means of two analyses.

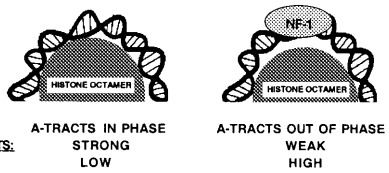

Figure 9. A model illustrating how DNA structure may modulate histone–DNA interaction and NF-1 accessibility for its nucleosomal binding site.

former construct. Further evidence that histone–DNA contacts are locally destabilized in ANoA3.5 comes from a comparison of the DNase I cutting patterns of the free and nucleosomal DNA segments within the NF-1 binding site of the different constructs (palindromic arrows in Figs 2A and B and 5). This reveals only subtle nucleosome-induced changes in the DNase I cutting pattern of the ANoA3.5 construct when compared with the two other constructs.

We found that NF-1 bound less strongly to ANiA3.5 than it bound to No4 (Fig. 6) and that less free DNA dissociated from the ANiA3.5 mononucleosome, as seen in electrophoretic mobility shift assays (Fig. 1C). The DNA curvature of ANiA3.5 was well maintained when compared with the curvature of No4 (Fig. 7) and the affinity of ANiA3.5 for histone octamer binding during nucleosome reconstitution was higher than it was for the ANoA3.5 construct (Fig. 8B). These results suggest that the DNA segment of the NF-1 site which is flanked by the two A-tracts bends smoothly around the histone octamer in ANiA3.5 and so facilitates histone–DNA contacts over the NF-1 site, while the opposite situation applies for ANoA3.5. A model illustrating these effects is shown in Figure 9.

The analysis of DNA curvature (Fig. 7) showed that the DNA of the No4 and ANiA3.5 constructs is curved along its entire length, whereas only the 3′-region of the ANoA3.5 construct is curved. The 5′-region of ANoA3.5 is noticeably uncurved. This argues strongly that DNA structural effects mediate the increased affinity for NF-1 of ANoA3.5. The DNA curvature analysis was performed with the program BEND (32) using an algorithm based on the *in vivo* nucleosome positioning data of Satchwell *et al.* (36). This algorithm was found to be the best in a comparison of several different algorithms for predicting DNA curvature (32). Furthermore, a strength of the algorithm is that since it is based on the nucleosome positioning data of Satchwell *et al.* (36), it should be particularly suitable for predicting the properties of DNA organized into nucleosomes.

DNA sequence is one of several important determinants influencing nucleosome positioning in the cell (39). There is a preferential distribution of GC-rich trinucleotides in the minor groove which face outwards and a preferential distribution of AT-rich trinucleotides in the minor groove which face towards the histone octamer surface. This, together with the fact that there is a period equal to the DNA helical repeat (40), was interpreted as a sequence pattern determining DNA curvature and thereby contributing to the stability of the nucleosome structure. Our results demonstrate that in a nucleosomal template, where DNA-bending motifs are distributed along the DNA double helix in such a way that they enhance a unidirectional bend around the histone octamer, DNA adopts a single rotational positioning with tight histone–DNA contacts. The opposite is also true: when DNA-bending motifs are not phased uniformly, nucleosomal DNA fails to adopt one single conformation and several rotational positionings are seen. Most importantly, in the latter case the nucleosomal DNA will be more accessible even for a DNA binding protein such as NF-1, which was previously reported to have a very low affinity for its nucleosomal DNA site irrespective of rotational positioning (4,12–14). This suggests that it is not a different rotational positioning, but a local decrease in contacts between histones and DNA, that results in the higher NF-1 binding affinity of ANoA3.5. However, we cannot exclude that NF-1 binding is also increased by certain rotational positions once the histone–DNA contacts have been reduced by the structure of the DNA.

Chromatin represses transcription *in vitro* (41) and *in vivo* (42,43). At least one of the mechanisms of repression is the restricted access of various transcription factors to their target DNA sites. Our results underscore the potentially wide range of affinities of NF-1 for its cognate binding site in a nucleosome context which may be obtained by differences in the local DNA sequence context. Several regulatory DNA segments harbor positioned nucleosomes (24,44). In such enhancers/promoters, a detailed understanding of

how different factors cooperate in gene regulation must include the effects of local sequence context and chromatin structure. A clear example of the positive effect of a single A-tract on gene regulation was recently given for the metal-responsive promoter of *Candida glabrata*. Here a positioned nucleosome was shown to harbor both a 16 bp A-tract and a metal-responsive element to which the metal-inducible transcription factor Amt1 binds in an A-tract-dependent fashion (45). A related study demonstrated that 17–42 bp long A-tracts stimulated transcription and increased DNA accessibility in chromatin *in vivo* (46). Our results show that short A-tracts can also have drastic effects on histone–DNA interactions and consequently on DNA accessibility.

ACKNOWLEDGEMENTS

We thank Ulla Björk for skillful technical assistance and Drs Tom Klenka and George Farrants for helpful corrections of the manuscript. We are grateful to Drs Jacky Schmitt and Hendrik Stunnenberg (EMBL, Heidelberg, Germany) for kindly providing recombinant vaccinia virus expressing NF-1 protein. We are indebted to Dr Björn Vennström and Kristina Nordström for help in growing and harvesting vaccinia-infected HeLa cells. We thank Dr David Goodsell for providing the BEND program and Alexey Kapranov for help in DNA curvature calculations. This work was supported by grants from the Swedish Cancer Foundation (grant 2222-B97-13XCC and a guest research fellowship to S.B. 3745-B97-02VAA), M.Bergwalls Foundation to Ö.W., R.Lundbergs Foundation and L.Hiertas Foundation and a graduate student fellowship from the Swedish Cancer Foundation (3211-B94-04UDD) to P.B.

REFERENCES

1 Luger,K., Mäder,A.W., Richmond,R.K., Sargent,D.F. and Richmond,T.J. (1997) *Nature*, **389**, 251–260.
2 Steger,D.J. and Workman,J.L. (1996) *BioEssays*, **18**, 875–884.
3 Perlmann,T. and Wrange,Ö. (1988) *EMBO J.*, **7**, 3073–3079.
4 Pina,B., Bruggemeier,U. and Beato,M. (1990) *Cell*, **60**, 719–731.
5 Li,Q. and Wrange,Ö. (1993) *Genes Dev.*, **7**, 2471–2482.
6 Pham,T.A., McDonnell,D.P., Tsai,M.-J. and O'Malley,B.W. (1992) *Biochemistry*, **31**, 1570–1578.
7 Wong,J., Shi,Y.-B. and Wolffe,A.P. (1995) *Genes Dev.*, **9**, 2696–2711.
8 Ng,K.W., Ridgway,P., Cohen,D.R. and Tremethick,D.J. (1997) *EMBO J.*, **16**, 2072–2085.
9 Taylor,I.C.A., Workman,J.L., Schuetz,T.J. and Kingston,R.E. (1991) *Genes Dev.*, **5**, 1285–1298.
10 Vettese-Dadey,M., Walter,P., Chen,H., Juan,L.J. and Workman,J.L. (1994) *Mol. Cell. Biol.*, **14**, 970–981.
11 Wechsler,D.S., Papoulas,O., Dang,C.V. and Kingston,R.E. (1994) *Mol. Cell. Biol.*, **14**, 4097–4107.
12 Archer,T.K., Cordingley,M.G., Wolford,R.G. and Hager,G.L. (1991) *Mol. Cell. Biol.*, **11**, 688–698.
13 Blomquist,P., Li,Q. and Wrange,Ö. (1996) *J. Biol. Chem.*, **271**, 153–159.
14 Eisfeld,K., Candau,R., Truss,M. and Beato,M. (1997) *Nucleic Acids Res.*, **25**, 3733–3742.
15 Imbalzano,A.N., Kwon,H., Green,M.R. and Kingston,R.E. (1994) *Nature*, **370**, 481–485.
16 Godde,J.S., Nakatani,Y. and Wolffe,A.P. (1995) *Nucleic Acids Res.*, **23**, 4557–4564.
17 Nowock,J., Borgmeyer,U., Püschel,A.W., Rupp,R.A.W. and Sippel,A.E. (1985) *Nucleic Acids Res.*, **13**, 2045–2061.
18 Kruse,U. and Sippel,A.E. (1994) *FEBS Lett.*, **348**, 46–50.
19 Santoro,C., Mermod,N., Andrews,P.C. and Tjian,R. (1988) *Nature*, **334**, 218–224.
20 de Vries,E., van Driel,W., van den Heuvel,S.J. and van der Vliet,P.C. (1987) *EMBO J.*, **6**, 161–168.
21 Mermod,N., O'Neill,E.A., Kelly,T.J. and Tjian,R. (1989) *Cell*, **58**, 741–753.
22 Meisterernst,M., Rogge,L., Foeckler,R., Karaghiosoff,M. and Winnacker,E.L. (1989) *Biochemistry*, **28**, 8191–8200.
23 Wu,L. and Whitlock,J.P. (1992) *Proc. Natl Acad. Sci. USA*, **89**, 4811–4815.
24 McPherson,C.E., Shim,E.-Y., Friedman,D.S. and Zaret,K.S. (1993) *Cell*, **75**, 387–398.
25 Cordingley,M.G., Riegel,A.T. and Hager,G.L. (1987) *Cell*, **48**, 261–270.
26 Truss,M., Bartsch,J., Schulbert,A., Hache,R.J.G. and Beato,M. (1995) *EMBO J.*, **14**, 1737–1751.
27 Vendetti,P., Di Croce,L., Kauer,M., Blank,T., Becker,P. and Beato,M. (1998) *Nucleic Acids Res.*, **26**, 3657–3666.
28 Shrader,T.E. and Crothers,D.M. (1989) *Proc. Natl Acad. Sci. USA*, **86**, 7418–7422.
29 Widlund,H.R., Simonsson,S., Magnusson,E.S.T., Nielsen,P.E., Kahn,J.D., Crothers,D.M. and Kubista,M. (1997) *J. Mol. Biol.*, **267**, 807–817.
30 Goodsell,D.S., Kopka,M.L., Cascio,D. and Dickerson,R.E. (1993) *Proc. Natl Acad. Sci. USA*, **90**, 2930–2934.
31 Gounari,F., De Francesco,R., Schmitt,J., van der Vliet,P.C., Cortese,R. and Stunnenberg,H. (1990) *EMBO J.*, **9**, 559–566.
32 Goodsell,D.S. and Dickerson,R.E. (1994) *Nucleic Acids Res.*, **22**, 5497–5503.
33 Lutter,L.C. (1978) *J. Mol. Biol.*, **124**, 391–420.
34 Riley,D. and Weintraub,H. (1978) *Cell*, **13**, 281–293.
35 McGhee,J.D. and Felsenfeld,G. (1979) *Proc. Natl Acad. Sci. USA*, **76**, 2133–2137.
36 Satchwell,S.C., Drew,H.R. and Travers,A.A. (1986) *J. Mol. Biol.*, **191**, 659–675.
37 Koo,H.-S., Wu,H.-M. and Crothers,D.M. (1986) *Nature*, **320**, 501–506.
38 Shrader,T.E. and Crothers,D.M. (1990) *J. Mol. Biol.*, **216**, 69–84.
39 Simpson,R.T. (1991) *Prog. Nucleic Acid Res. Mol. Biol.*, **40**, 143–184.
40 Drew,H.R. and Travers,A.A. (1985) *J. Mol. Biol.*, **186**, 773–790.
41 Kraus,W.L. and Kadonaga,J.T. (1998) *Genes Dev.*, **12**, 331–342.
42 Han,M., Kim,U.-J., Kayne,P. and Grunstein,M. (1988) *EMBO J.*, **7**, 2221–2228.
43 Perlmann,T. and Wrange,Ö. (1991) *Mol. Cell. Biol.*, **11**, 5259–5265.
44 Richard-Foy,H. and Hager,G.L. (1987) *EMBO J.*, **6**, 2321–2328.
45 Zhu,Z. and Thiele,D.J. (1996) *Cell*, **87**, 459–470.
46 Iyer,V. and Struhl,K. (1995) *EMBO J.*, **14**, 2570–2579.